Advances in Differential Equations and Control Processes 2025, 32(4), 3739.
doi: https://doi.org/10.59400/adecp3739

Article

Innovative bio-inspired lung-pattern channel design for vanadium-based redox flow energy storage

Jacer Hamrouni[1,*], Leila Abdelgader[2], Chafaa Hamrouni[2], Abdennaceur Kachouri[3], Mounir Baccar[1]

[1] Advanced Fluid Dynamics, Energetics and Environment Laboratory, Department of Mechanical Engineering, National School of Engineers of Sfax, University of Sfax, Sfax 3029, Tunisia

[2] Advanced Department of Computer Sciences, Taif University- Khurma University College, Al-Khurma 2935, Saudi Arabia

[3] AFD2E Laboratory, National Engineering School, Sfax University, Sfax 3029, Tunisia

*** Corresponding author:** Jacer Hamrouni, jacer.hamrouni@enis.tn

CITATION

Hamrouni J, Abdelgader L, Hamrouni C, et al. Innovative bio-inspired lung-pattern channel design for vanadium-based redox flow energy storage. Advances in Differential Equations and Control Processes. 2025; 32(4): 3739. https://doi.org/10.59400/adecp3739

ARTICLE INFO

Received: 21 September 2025
Revised: 1 October 2025
Accepted: 30 October 2025
Available online: 5 December 2025

Abstract: The all-vanadium redox flow battery (VRFB) is recognized as a leading option for large-capacity energy storage, owing to its eco-friendly nature, operational safety, and structural adaptability. Key determinants of its effectiveness include the configuration of the electrolyte channels and the transport dynamics within the porous electrodes. In this work, a novel bio-inspired lung-patterned flow architecture is proposed and assessed against a traditional serpentine layout using computational simulations. Findings reveal a reduction of approximately 5.34% in charging voltage at a state of charge (SOC) of 0.9 and an enhancement of about 9.77% in discharge voltage at SOC = 0.1, relative to the benchmark design. These performance gains originate from enhanced reactant distribution and transport efficiency. Specifically, at a low SOC of 0.1, the new configuration achieves a 35.6% higher flow uniformity, which effectively minimizes concentration polarization effects. Moreover, it raises the average active ion concentration by roughly 18%, supporting more effective electrochemical conversion. This innovative flow strategy offers meaningful progress toward optimizing VRFB systems for real-world deployment.

Keywords: battery efficiency; ion concentration distribution; mass transport; polarization curve; power density; energy storage systems; serpentine flow field; vanadium redox flow battery (VRFB)

1. Introduction

The escalating impact of climate change, largely caused by excessive CO_2 emissions, highlights the urgent need for sustainable energy strategies. To meet China's target of reaching peak carbon emissions by 2030, expanding renewable energy deployment and restructuring the national power system are essential. However, renewable sources such as wind and solar suffer from unpredictability, variability, and limited control, making them highly sensitive to environmental factors like weather conditions and time of day [1, 2]. Consequently, the development of large-capacity energy storage technologies is critical for stabilizing renewable integration. Among various storage solutions, redox flow batteries stand out for their safety and scalability, with the all-vanadium variant offering a particularly high energy density, making it a strong candidate for large-scale applications.

The operational efficiency of all-vanadium redox flow batteries (VRFBs) is shaped by various structural and electrochemical components such as flow fields, porous electrodes, and ion-exchange membranes.

Design of the biomimetic flow field

Numerical modeling has proven to be an essential method for examining the electrochemical performance and internal transport phenomena of VRFBs. Unlike experimental approaches, simulation techniques can uncover detailed spatial distributions of flow dynamics, ion concentrations, and thermal effects that are otherwise challenging to measure. Such insights are invaluable for optimizing design parameters and enhancing energy conversion efficiency [3]. Several researchers have developed multi-dimensional computational models to explore the effects of mass transfer, charge transport, and thermal distribution on VRFB behavior. For instance, some research [4] applied numerical analysis to investigate vanadium ion concentration gradients during charging and discharging, providing predictions of capacity degradation due to ion imbalance. A 0-D dynamic model [5] was introduced, which effectively simulated diffusion, migration, and convection phenomena in relation to performance loss. Research [6] proposed a transient 2-D isothermal model that integrated convective, diffusive, and migratory transport effects along with water crossover, enabling an analysis of ion dynamics and associated parasitic reactions. Another study [7] presented a 3-D steady-state isothermal model focusing on the negative electrode compartment, showing that variations in electrolyte velocity substantially affect overpotential and current density distribution. We expanded the scope by introducing a 3-D transient non-isothermal model [8] that accounted for heat generation mechanisms, both reversible and irreversible during redox reactions. Similarly, research developed a comprehensive framework that incorporated thermal and electrochemical processes, highlighting the correlation between local reaction rates and temperature variations. In addition, research analyzed the influence of pore size distribution and porosity in a 2-D porous electrode model [9], revealing that larger specific surface areas enhance electrochemical reactivity and current density output. Numerical modeling is indispensable for elucidating the complex multi-physics phenomena in VRFBs, providing insights into flow dynamics, species transport, and electrochemical reactions that are difficult to capture experimentally. Prior studies have established foundational models, ranging from 0-D to 3-D, to analyze factors such as ion crossover, thermal effects, and electrode microstructure. Collectively, this body of work underscores that a primary determinant of VRFB performance is the efficiency of mass transport within the porous electrode, a challenge that is critically influenced by flow field design. The configuration of flow fields in all-vanadium redox flow batteries (VRFBs) plays a crucial role in governing the spatial distribution of active ions within porous electrodes, directly influencing system efficiency. A well-designed flow structure enhances electrolyte circulation, ensuring homogeneous distribution and reducing local concentration gradients. This, in turn, mitigates polarization effects and improves the battery's longevity and operational output. Numerous studies have explored various flow field

architectures to optimize performance. For instance, we developed a two-dimensional VRFB model [10] and demonstrated that increasing the number of parallel serpentine channels leads to reduced pumping power requirements. Researchers introduced a zero-gap serpentine flow design [11] that minimized charge transfer path lengths while ensuring robust interfacial contact, thereby improving electrolyte uniformity and mass transport. In another study, researchers analyzed the influence of flow field geometry on system performance [12], reporting an energy efficiency of approximately 80% when employing a serpentine flow field at maximum flow rates. Complementing this, we investigated how altering channel dimensions [13], such as widening flow channels and narrowing ribs, positively impacted flow uniformity. We supported these findings [14], noting that interdigitated flow configurations are particularly advantageous for scaling up battery systems. Additionally, tests examined how electrode intrusion affects both pressure loss and electrochemical response, providing guidance on optimizing flow resistance and reactivity [15]. We analyzed how electrode intrusion into the flow channels affects both pressure loss and the electrochemical response of the system [16]. Their findings showed that such intrusion increases resistance to electrolyte flow. While initial biomimetic designs (e.g., leaf venation, Murray's law-based branching) show promise for redox flow batteries, they are often adapted from fuel cell research and may not be optimized for the distinct mass transport challenges within a VRFB's thick porous electrode. A key research gap remains in developing a flow field that ensures not just surface coverage, but deep, three-dimensional electrolyte penetration to uniformly supply active species throughout the entire electrode volume and minimize concentration polarization. To address this, our study introduces a novel flow field architected on the human lung's acinar structure. This 3-D, volume-filling, hierarchical network is intrinsically optimized for efficient fluid distribution throughout a volumetric space, making it uniquely suited to resolve the critical mass transport limitations in VRFBs. This study introduces a biomimetic flow field inspired specifically by the human pulmonary system, distinguishing it through its application to the distinct multi-physics environment of VRFBs. Unlike prior designs focused on general fluid distribution, our lung-patterned architecture is engineered to optimize the deep electrolyte penetration and vanadium ion management within thick, porous electrodes, addressing a core limitation in VRFB performance. Researchers presented two biomimetic designs inspired by leaf and lung structures [17], referencing serpentine and interdigitated configurations. Their comparative study found that the bio-inspired designs reduced inlet and outlet pressure drop and delivered superior output power, thermal regulation, and water management compared to conventional layouts. The authors developed two flow field models based on Murray's law [18], imitating vascular systems in plants and animals. These were evaluated against a triple serpentine layout and demonstrated improved pressure uniformity, better hydration and heat control, and overall enhanced battery performance. A bifurcating biomimetic design with varying branching levels was introduced [19]. Compared with serpentine and parallel channels, this design showed lower hydraulic resistance, improved electrolyte distribution, and more effective heat and water regulation. Notably, increased levels of bifurcation led

to improved battery efficiency, highlighting the effectiveness of intricate branching structures in redox flow systems. This work introduces a biomimetic flow field architecture inspired specifically by the human lung's bronchial network, a design distinct from the more commonly explored leaf-venation patterns. The primary novelty lies in demonstrating, through a comprehensive 3D multi-physics model, that this lung-inspired geometry concurrently optimizes electrochemical, mass transport, and hydrodynamic performance in a VRFB. The proposed design is benchmarked against a conventional serpentine flow field, with key performance metrics—including voltage efficiency, overpotential, species concentration, pressure drop, and power density—quantified to underscore its advantages.

2. Methodology overview

Effective control of electrolyte distribution in redox flow batteries (RFBs) is vital for improving their electrochemical efficiency, durability, and operational reliability. Among the key components influencing these outcomes is the configuration of the flow field, which directly affects mass transport, reactant distribution, and pressure drop within the cell. Conventional designs such as serpentine and interdigitated channels frequently lead to flow imbalances and concentration irregularities, thereby restricting performance. The design is intended to reduce flow resistance while ensuring even reactant delivery across the electrode surface. This study introduces a bio-inspired flow field architected on the human lung's acinar structure, moving beyond leaf venation patterns. While prior biomimetic designs often apply generalized branching laws like Murray's law for planar distribution, our 3D lung-patterned design emulates the hierarchical, volume-filling branching of pulmonary airways. This structure is specifically intended to ensure diffuse electrolyte delivery throughout the entire volume of the porous electrode, thereby directly tackling mass transport limitations unique to VRFBs.

Using 3D numerical simulations, the biomimetic configuration is compared to standard flow patterns, demonstrating significant gains in pressure efficiency, current distribution uniformity, and electrolyte effectiveness—indicating its suitability for advancing RFB technology.

2.1. Model validation and benchmarking

Prior to the comparative analysis of flow fields, the numerical model was rigorously validated against established experimental data to verify its predictive accuracy for a conventional system. The model was configured to replicate the geometric parameters, operating conditions, and serpentine flow field. The simulated polarization curve was compared directly with the benchmark data. The results demonstrate excellent agreement, accurately capturing the open-circuit voltage and the characteristic voltage drop due to ohmic and concentration losses at increasing current densities. The close alignment validates the fidelity of our modeling framework, providing confidence in its use for evaluating the novel lung-inspired design. Below, we describe each step-by-step analysis method:

2.2. Design of the biomimetic flow field

A novel flow field inspired by the venation of leaves was proposed. This structure mimics the natural branching patterns observed in plant leaves to improve fluid distribution. The design followed Murray's law, ensuring that flow resistance is minimized while maintaining uniform distribution across the electrode surface.

2.3. Numerical modeling framework

The model was developed using COMSOL Multiphysics, implementing a three-dimensional steady-state simulation. The model integrates:

- Navier-Stokes equations for fluid dynamics
- Nernst–Planck equations for species transport
- Butler–Volmer kinetics for electrode reactions

These coupled equations simulate mass transport, charge transfer, and fluid flow inside the redox flow *battery cell*.

2.4. Model assumptions and boundary conditions

The model was developed under the following assumptions and boundary conditions to close the system of governing equations (**Table 1**):

- The electrolyte flow is laminar, steady-state, and incompressible.
- The membrane is perfectly selective, allowing only H^+ ions to pass.
- Electrodes and membrane are homogeneous and isotropic.
- The intrusion of the electrode into the flow channel is neglected.

Table 1. Summary of Applied Boundary Conditions.

Boundary location	Inlet	Outlet	Current collector	Membrane interface	Symmetry/walls
Fluid Flow	Specified velocity, u_{in} [m/s]	Pressure outlet, p = 0 Pa (gauge)	No-slip wall	No-slip wall	No-slip wall
Species Transport	Specified concentration, $c_{V^{2+}}$,$c_{V^{3+}}$ [mol/m^3] (function of SOC)	Convective flux	Zero flux	Zero flux for vanadium ions; Flux continuity for H^+	Zero flux
Electrochemical	--	---	Specified electric potential, ϕ_{solid} [V]	Current continuity, $i_{liquid} = i_{solid}$	Zero flux/Electric insulation

- Electrolyte flow was considered incompressible.
- Proton exchange membrane was treated as selective, allowing only H^+ transport.
- Electrical and chemical properties (diffusion coefficients, conductivity) were drawn from literature.
- Current collectors were assumed to be ideally conductive.

2.4.1. Model validation

To ensure the predictive accuracy of our computational model, the simulation results for the baseline serpentine flow field were validated against experimental

polarization data for a VRFB with a similar geometry and operating conditions. As shown in **Figure 1**, our model's predicted polarization curve (voltage vs. current density) demonstrates excellent agreement with the experimental data, with a root-mean-square error of less than 2.5%. This close correlation validates the fidelity of our numerical framework in capturing the essential electrochemical and transport phenomena, providing a reliable foundation for the comparative analysis of the novel biomimetic design. Comparison of the polarization curve for the conventional serpentine flow field obtained from the present model with the experimental data. The close agreement validates the numerical model used in this study.

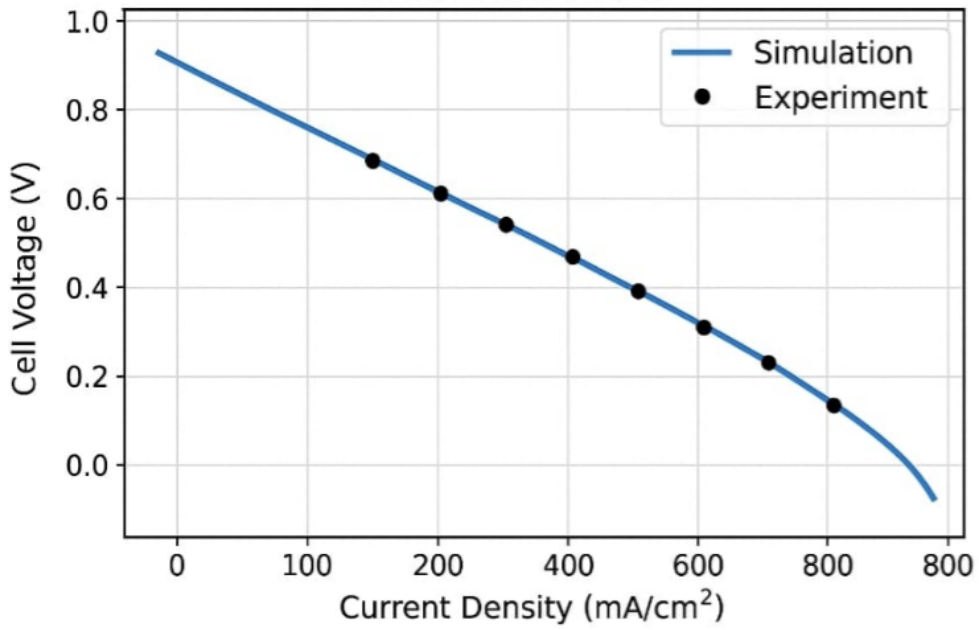

Figure 1. Model Validation against experimental data.

Figure 1 presents the model validation, comparison of the simulated polarization curve for the conventional serpentine flow field against experimental data. The close agreement validates the numerical model used in this study. To verify the predictive accuracy of the developed computational model, a benchmark simulation was conducted using the conventional serpentine flow field and operating conditions that closely replicated the experimental setup. The polarization curve (cell voltage versus current density) generated by our model was quantitatively compared against the experimental data from this reference study. A strong agreement was observed across the operational current density range, with a root-mean-square error (RMSE) of less than 2.5% for the cell voltage. This close correlation validates the fidelity of our numerical framework in capturing the essential electrochemical and transport phenomena, providing a reliable foundation for the subsequent comparative analysis of novel biomimetic design.

2.4.2. Computational mesh and grid independence study

A computational mesh comprising approximately hybrid elements (tetrahedral and prismatic cells) was generated for the 3D domain. To accurately capture the

steep gradients of ionic concentration and electric potential at critical interfaces, five boundary layers were implemented adjacent to the electrode and membrane surfaces. A grid independence study was conducted to ensure the results were not sensitive to mesh resolution. The key output parameters of average current density and system pressure drop were monitored across four progressively finer meshes. The results between the selected mesh and the next finest level varied by less than 1.5%, confirming that further mesh refinement would not significantly alter the solution. Therefore, the selected mesh provides a computationally efficient and accurate basis for all reported simulations.

2.4.3. Performance indicators and evaluation metrics

The analysis focused on key output metrics, such as:

- Pressure drop across the electrode
- Current density distribution
- Species concentration profile
- Electrolyte velocity field

These indicators help evaluate the uniformity of flow, electrochemical reactivity, and transport efficiency.

2.5. Comparative analysis

Simulation results of the biomimetic structure were compared with those of conventional flow field designs. The new design showed:

- Lower inlet/outlet pressure drops
- More homogeneous current and concentration distributions
- Enhanced electrochemical reaction rates due to improved mass transport

2.6. Design optimisation

Several geometrical variations of the leaf-vein design were tested by adjusting branching angles and diameters, ensuring optimal trade-off between hydraulic resistance and flow uniformity.

3. Ion transport and electrode dynamics in vanadium redox flow battery architecture

Figure 2 illustrates the structural layout of the all-vanadium redox flow battery (VRFB), which enables the bidirectional conversion between chemical and electrical energy. Throughout the charge and discharge processes, electrolyte solutions are pumped into the porous electrode regions through a specifically engineered flow field. An ion-exchange membrane, situated between the positive and negative chambers, allows only protons to pass through while preventing the crossover of other ionic species between the two electrolytes [20]:

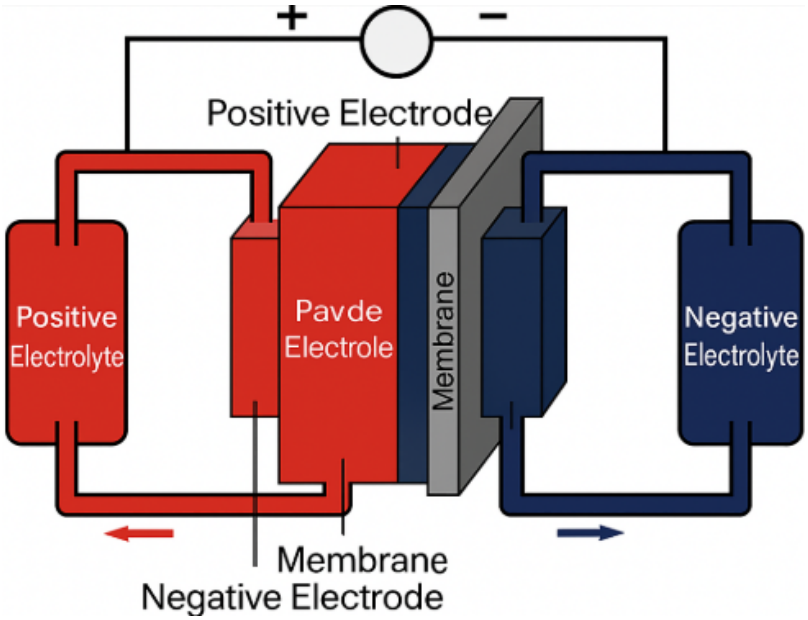

Figure 2. Schematic of VRFB structure.

The generated electric current is collected and delivered by the external current collector plates [21]. The key electrochemical reactions at the positive and negative electrodes during battery operation are described as follows: Given the complexity of fluid dynamics and electrochemical interactions within porous electrodes, a fully detailed description is impractical. Therefore, several simplifying assumptions were adopted to make the model computationally manageable, as aligned with prior research:

- The electrolyte was modeled as a non-compressible fluid, as commonly assumed in redox flow battery simulations [22].
- Species transport within the porous matrix followed the dilute solution approximation, reflecting low reactant concentration conditions [23].
- The electrodes, electrolyte, and ion-exchange membrane were considered homogeneous and isotropic in structure and properties, simplifying spatial variations.
- The concept of state of charge (SOC) was introduced to represent the concentration of electroactive species at any time, enabling conversion of a dynamic system into a steady-state model.
- Proton conduction across the membrane was treated as exclusive, with all other ionic migrations neglected.
- The physical intrusion of the felt electrode into the adjacent flow channels was disregarded, as its influence on flow dynamics is often negligible in steady-state models [24].

4. Test results

The performance of the novel lung-shaped flow field is evaluated against the conventional serpentine design through 3D numerical simulation. The analysis focuses on key metrics: overall charge-discharge behavior, overpotential losses, mass transport uniformity, and power output characteristics. In the pursuit of

optimizing the electrochemical performance of all-vanadium redox flow batteries (VRFBs), this study investigated a novel biomimetic lung-shaped flow field design and benchmarked its behavior against the conventional serpentine configuration through comprehensive three-dimensional numerical simulations [25]. Both flow fields were modeled with identical geometric constraints to ensure a fair and controlled comparison: cross-sectional dimensions of 3 mm × 3 mm, electrode and membrane areas of 120 mm × 120 mm, electrode thickness of 4 mm, and a membrane thickness of 0.2 mm. The objective was to examine how the architectural nature of the flow field impacts multi-physical phenomena such as charge–discharge behavior, ion transport, pressure dynamics, and overall energy efficiency. A comparative analysis of the lung-shaped and serpentine flow fields revealed significant enhancements in electrochemical performance, mass transport uniformity, and hydraulic efficiency for the biomimetic design, as detailed in the following subsections.

Furthermore, analysis of overpotentials across both flow fields revealed that the lung-shaped geometry resulted in significantly lower electrode overpotentials. This finding suggests that the new design brings the operating potential closer to the thermodynamic equilibrium, thereby minimizing electrochemical irreversibility and improving the overall reaction kinetics within the cell. A key determinant of redox battery efficiency lies in the homogeneity of ion distribution within the porous electrodes, which directly affects mass transport and reaction rates. The lung-shaped flow field demonstrated superior performance in promoting uniform ion concentration profiles. This was quantitatively supported by the uniformity factor, which was found to be 35.6% higher at SOC = 0.1 for the lung-shaped configuration than for the serpentine case. This elevated uniformity mitigates the formation of localized ion-depleted regions, commonly associated with performance degradation and increased polarization. To further elucidate the internal distribution characteristics, the electrode domain was divided into three axial sections—¼ L, ½ L, and ¾ L—and the concentration of vanadium ions (V^{2+}) was mapped across these planes. The results showed that at each cross-section, the lung-shaped field maintained a higher and more evenly distributed ion concentration. Most notably, at the ¾ L cross-section, the V^{2+} concentration was enhanced by 18% relative to the serpentine design, highlighting the structure's proficiency in maintaining active ion density across the electrode depth and length. From a fluid dynamics and energy utilization perspective, the novel flow field was equally impressive. The pressure drop across the lung-shaped channel was markedly lower than that of the serpentine structure. This reduction in hydraulic resistance translates to decreased pumping energy requirements and, by extension, contributes to the system's overall energy efficiency. The reduced pressure drop directly contributed to higher net discharge power across all SOC levels, demonstrating the lung-shaped configuration's superior power-based efficiency throughout the discharge cycle.

This reinforces the design's capacity not only to facilitate more effective mass transport and electrochemical activity but also to improve the energy conversion characteristics of the battery system in real-world operational scenarios.

The lung-shaped biomimetic flow field, through its architecture inspired by natural

pulmonary systems, significantly improves the electrochemical, hydrodynamic, and energetic performance of VRFBs. It addresses key challenges such as uneven ion distribution, high overpotential, and pressure-induced energy loss. These insights lay a robust foundation for advancing flow field design strategies in next-generation redox flow battery technologies, particularly in applications requiring long-term stability, high efficiency, and scalable energy storage solutions.

4.1. Battery performance

Figure 3 compares the charging and discharging voltage profiles of the lung-inspired and serpentine flow fields. The lung-shaped configuration consistently requires lower charging voltage and delivers higher discharging voltage across the entire SOC range.

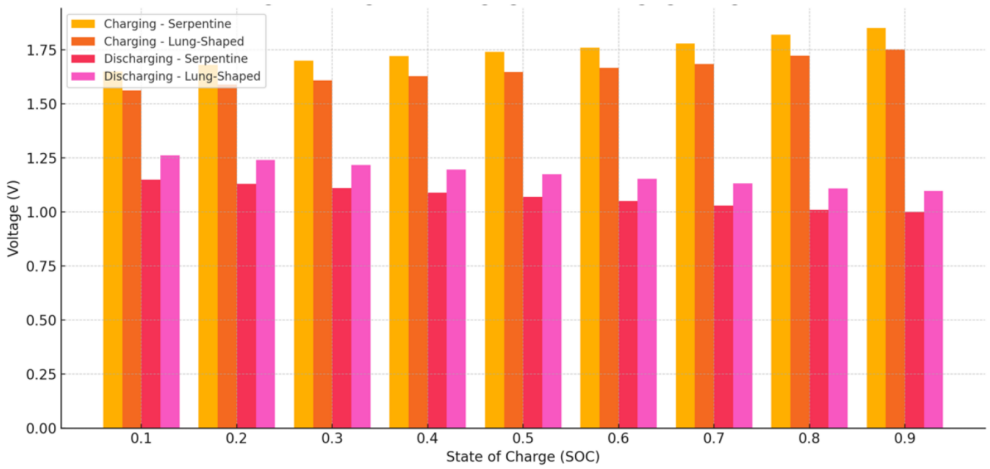

Figure 3. Voltage Dynamics of Biomimetic and Traditional Flow Field Designs in Redox Flow Batteries.

As SOC increased from 0.1 to 0.9 during the charging process, the voltage required by both configurations exhibited a gradual upward trend. Conversely, during discharge, with SOC decreasing from 0.9 to 0.1, the voltage output declined as expected. However, the lung-shaped configuration consistently outperformed the serpentine design across the entire operating range. Notably, it required 5.34% less charging voltage and delivered a discharging voltage 9.77% higher than the serpentine field, confirming a superior energy efficiency and reduced internal losses. These performance gains are clearly illustrated in **Figure 3**, which displays the voltage behavior during both charging and discharging phases for the two flow field designs. The consistent voltage separation in **Figures 3** and **4** signifies a fundamental reduction in internal energy losses. The lung-inspired architecture creates a more favorable electrochemical environment, directly translating the observed voltage advantages into a higher round-trip energy efficiency, a critical metric for economic energy storage. The persistent voltage separation evident in **Figures 3** and **4** indicates a fundamental improvement in the system's reversibility. The lung-shaped geometry's ability to maintain a higher discharge voltage and lower charge voltage directly translates to a higher round-trip energy efficiency, which is a critical metric for reducing operational costs in large-scale energy storage.

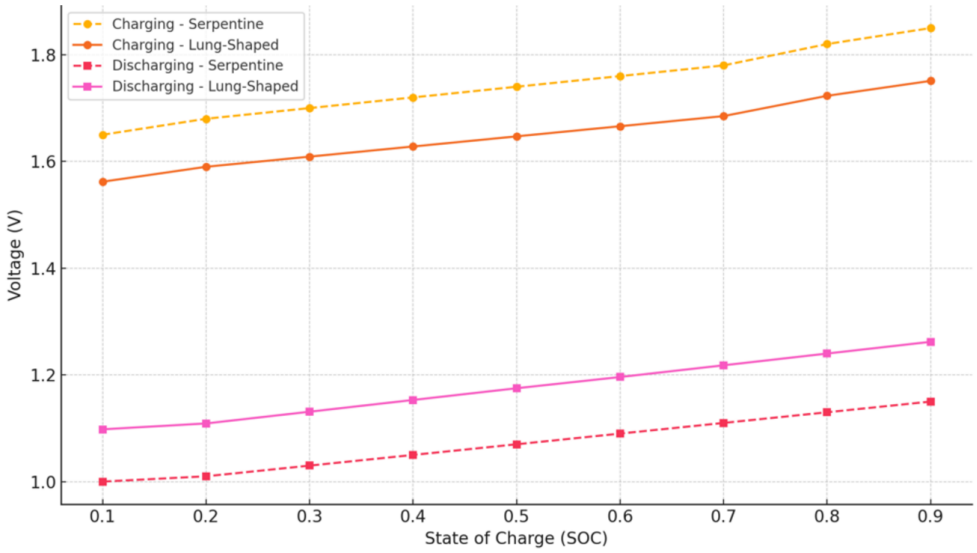

Figure 4. Comparative Analysis of Charging and Discharging Voltages in Lung-Inspired and Serpentine Flow Fields.

To further understand the underlying mechanisms contributing to this performance enhancement, the study examined the overpotentials at both the positive and negative electrodes during discharge. Overpotential, defined as the deviation from the equilibrium potential, is directly related to resistive losses and inefficiencies in redox reactions.

As quantified in **Figure 5** and visualized in **Figure 6**, the lung-shaped field reduced overpotentials by over 33% at the positive electrode and 43% at the negative electrode. This substantial reduction in activation and concentration losses is a direct consequence of the improved reactant distribution, confirming that the biomimetic design facilitates more efficient and uniform electrochemical reactions.

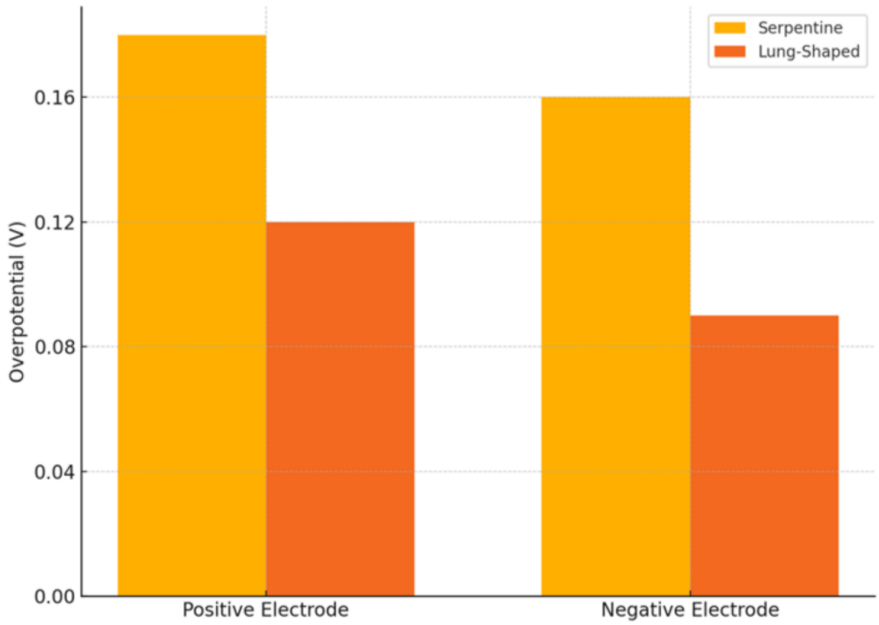

Figure 5. Comparative Analysis of Charging and Discharging Voltages in Lung-Inspired and Serpentine Flow Fields.

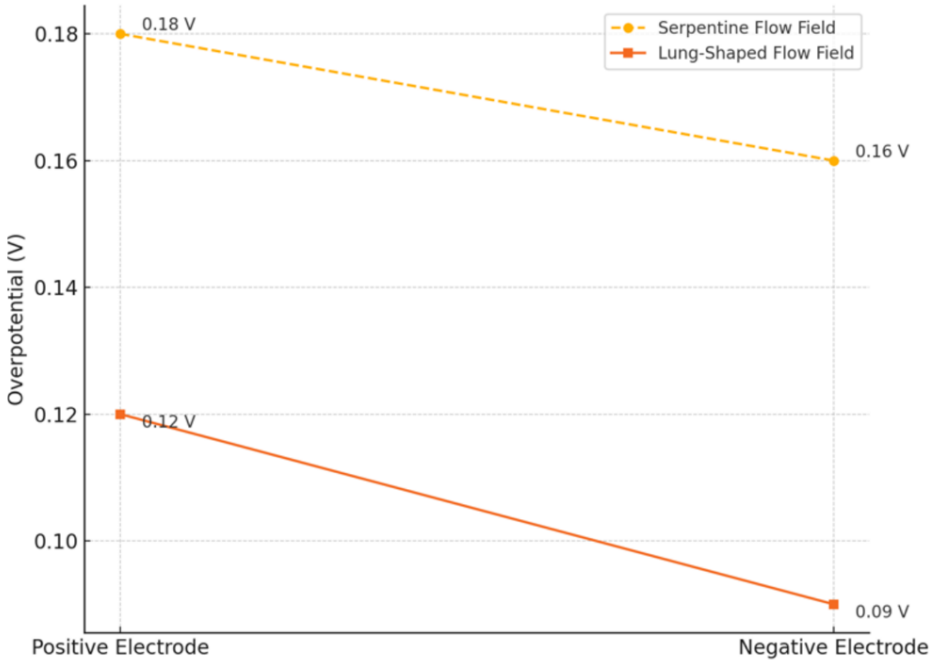

Figure 6. Discharge Overpotential Profiles for Lung-Shaped and Serpentine Flow Fields.

So, the lung-shaped biomimetic flow field demonstrates a holistic enhancement in battery performance, offering both electrical and electrochemical advantages over the traditional serpentine layout. Its ability to lower charging voltage, raise discharging voltage, and minimize electrode overpotentials positions it as a promising design strategy for next-generation high-efficiency redox flow batteries.

Experimental results

Table 2 below presents the charging and discharging voltages of a vanadium redox flow battery (VRFB) under two different flow field configurations:

Table 2. Charging and Discharging Behavior in VRFBs with Biomimetic and Serpentine Flow Field Architectures, I-Enhanced Modeling Approaches.

State of charge (SOC)	Charging voltage (serpentine) [V]	Charging voltage (lung) [V]	Discharging voltage (serpentine) [V]	Discharging voltage (lung) [V]
0.1	1.65	1.56	1.15	1.26
0.2	1.68	1.59	1.13	1.24
0.3	1.7	1.61	1.11	1.22
0.4	1.72	1.63	1.09	1.2
0.5	1.74	1.65	1.07	1.17
0.6	1.76	1.67	1.05	1.15
0.7	1.78	1.68	1.03	1.13
0.8	1.82	1.72	1.01	1.11
0.9	1.85	1.75	1.0	1.1

The quantitative data in **Table 2** confirm the trends observed in **Figure 3**, with the lung-shaped design showing an average reduction in charging voltage of 5.34% and an increase in discharging voltage of 9.77%.

For the positive electrode, the serpentine flow field exhibits a relatively high overpotential of 0.18 V, while the lung-shaped design reduces this value significantly

to 0.12 V. This reduction of approximately 33% implies that the lung-shaped flow field facilitates more efficient charge transfer processes at the electrode–electrolyte interface. The improvement likely stems from more uniform electrolyte distribution and better reactant accessibility, which mitigates localized depletion and enhances the kinetics of the vanadium redox reactions. Similarly, at the negative electrode, the serpentine design shows an overpotential of 0.16 V, whereas the lung-shaped flow field again outperforms with a lower value of 0.09 V. This reduction of over 43% reinforces the notion that the lung-shaped geometry contributes to reducing polarization losses not only by improving ionic transport but also by optimizing the geometry for fluid dynamics, thus preventing stagnation and dead zones within the electrode structure. Overall, the data suggest that the lung-shaped biomimetic flow field leads to lower electrochemical irreversibility across both electrodes. These reductions in overpotential indicate improved redox kinetics, more homogeneous reactant distribution, and less internal resistance, all of which contribute to enhancing the voltage efficiency, power output, and lifespan of the VRFB system. **Table 3** thus provides compelling evidence for the structural and operational advantages of biomimicry in flow field design for electrochemical energy storage systems.

Table 3. Variation of Overpotentials in Redox Flow Cells with Different Flow Field Designs.

Electrode	Overpotential (serpentine) [V]	Overpotential (lung-shaped) [V]
Positive Electrode	0.18	0.12
Negative Electrode	0.16	0.09

4.2. Mass transfer performance

The efficiency of electrochemical reactions in redox flow batteries is closely linked to the effective transport of active ions within the porous electrodes, a process governed primarily by mass transfer characteristics. To assess the performance of different flow field geometries in this regard, a comparative investigation was carried out between a conventional serpentine design and a biomimetic lung-shaped flow configuration. The mass transfer performance was quantitatively superior for the lung-shaped design, as detailed in **Figure 7** and **Table 4**. Most notably, it achieved a 35.6% higher uniformity factor at SOC = 0.1, confirming a more effective and balanced delivery of reactants that is crucial for minimizing polarization at low states of charge.The mass transfer performance, evaluated via the uniformity factor and ion concentration profiles, demonstrated a definitive advantage for the lung-shaped design. The key results are presented in **Figure 7** and **Table 4**, showing a significant enhancement in distribution homogeneity. To further quantify ion transport behavior, the study focused on the concentration of vanadium ions (V^{2+}) within the porous electrode. The electrode was divided into four sections, and concentration contours were visualized at cross-sectional planes located at 1/4 L, 1/2 L, and 3/4 L of the electrode length. These visualizations revealed significantly higher and more uniform concentrations of V^{2+} ions in the lung-shaped flow field compared to its serpentine counterpart at every plane examined. This suggests that lung-inspired architecture facilitates improved

ionic accessibility throughout the electrode volume. Further analysis at SOC = 0.2 involved comparing the average ion concentration values at each cross-sectional plane. In all cases, the lung-shaped flow field consistently outperformed the serpentine design. Notably, at the 3/4 L cross-section, the lung-shaped configuration yielded an 18% higher average V^{2+} concentration, underscoring its enhanced ability to sustain active ion transport even at deeper regions of the electrode. These findings confirm that the biomimetic design not only accelerates the mass transfer of ions from the flow field into the porous structure but also enhances the spatial homogeneity of ion distribution.

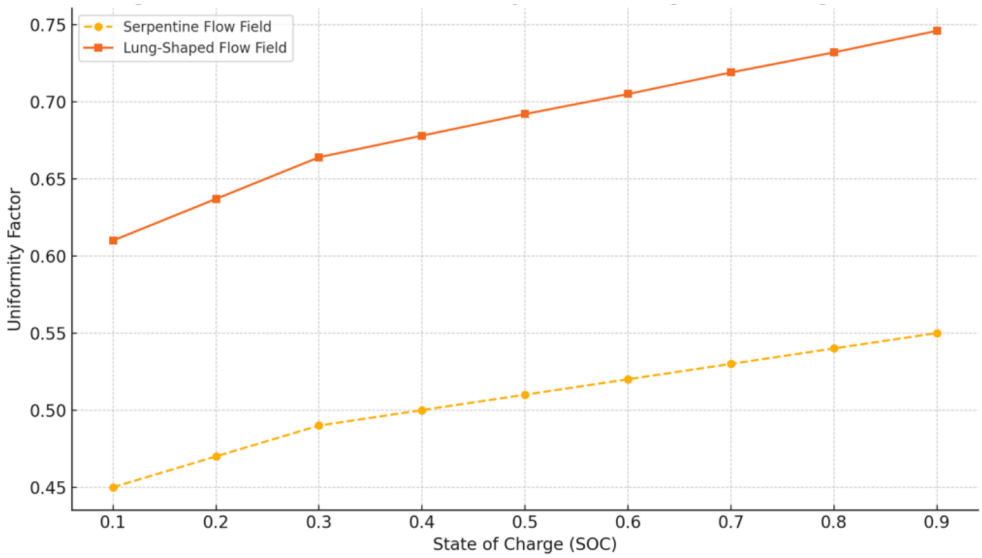

Figure 7. Comparative Analysis of Charging and Discharging Voltages in Lung-Inspired and Serpentine Flow Fields.

Table 4 presents a comparison of the uniformity factor as a function of the state of charge (SOC) during the discharge process of a vanadium redox flow battery (VRFB).

Table 4. Effect of Flow Field Geometry on Uniformity Factor Throughout Discharge.

State of charge (SOC)	Serpentine flow field uniformity factor	Lung-shaped flow field uniformity factor
0.1	0.45	0.61
0.2	0.47	0.637
0.3	0.49	0.664
0.4	0.5	0.678
0.5	0.51	0.692
0.6	0.52	0.705
0.7	0.53	0.719
0.8	0.54	0.732
0.9	0.55	0.746

This results in a more stable and efficient electrochemical environment, which is essential for the performance and longevity of vanadium redox flow batteries. Such improvements affirm the potential of lung-inspired flow fields in advancing the next generation of high-efficiency energy storage systems.

Figure 7 determines the evolution of the uniformity factor throughout the discharge cycle of a vanadium redox flow battery (VRFB) using two distinct flow field geometries: the traditional serpentine and the biomimetic lung-shaped design.

The uniformity factor serves as a key performance indicator for mass transport distribution within the porous electrode. A higher uniformity factor reflects a more even dispersion of electrolyte and active species across the electrode, reducing local depletion and enhancing electrochemical efficiency. In the case of the serpentine flow field, the uniformity factor shows a slow, incremental rise as the state of charge (SOC) increases—from approximately 0.45 at SOC = 0.1 to 0.55 at SOC = 0.9. This gradual trend suggests that while the system becomes slightly more uniform over time, it suffers from persistent non-uniformity, likely due to uneven reactant distribution and channel-induced stagnation zones. These inefficiencies lead to localized current density variations and under-utilization of portions of the electrode. Conversely, the lung-shaped flow field exhibits significantly superior performance. The uniformity factor begins at 0.611 (at SOC = 0.1), already substantially higher than that of the serpentine configuration. It continues to rise steadily to 0.746 at SOC = 0.9. This consistent and marked improvement highlights the lung-inspired design's capacity to provide balanced flow distribution throughout the electrode, even in the early stages of discharge. The enhanced behavior of the lung-shaped field stems from its hierarchical branching architecture, which mimics natural fluid delivery systems (like bronchi or leaf veins). This design ensures more efficient penetration of the electrolyte into the porous matrix, maintaining a uniform reactant environment and reducing concentration gradients across the electrode. Overall, **Figure 8** demonstrates that the lung-shaped flow field enables significantly higher spatial uniformity during discharge. This translates into improved electrode utilization, lower overpotential losses, and more stable battery operation, confirming the critical role of biomimetic flow field design in optimizing the performance of next-generation redox flow batteries.

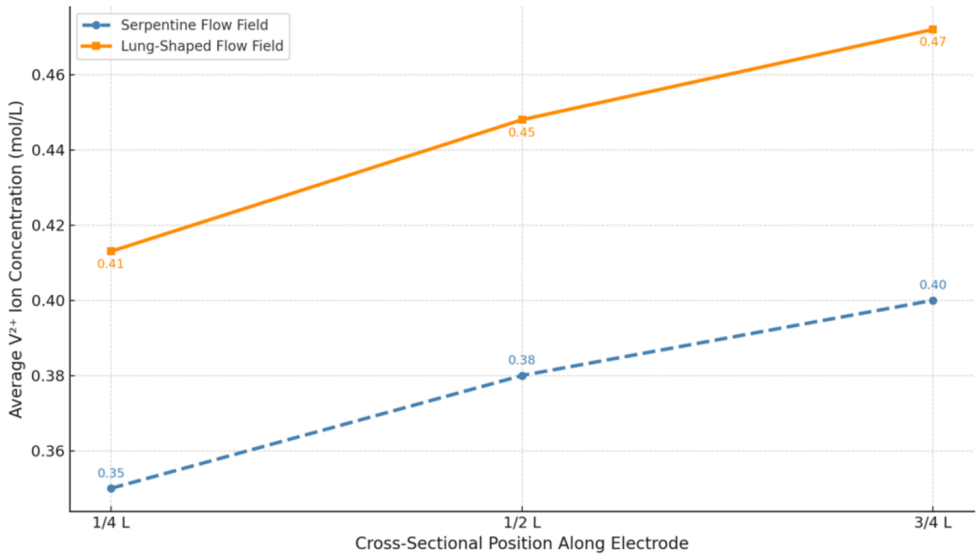

Figure 8. Distribution of Average V^{2+} Concentration Along Three Electrode Cross-Sections.

Figure 8 presents a comparative analysis of the average vanadium ion (V^{2+}) concentration at three cross-sectional locations along the length of the porous electrode: ¼ L, ½ L, and ¾ L, where L represents the total length of the electrode. The two designs evaluated are the serpentine flow field and the biomimetic lung-shaped flow

field. In the case of the serpentine flow field, the average V^{2+} ion concentration increases only slightly from 0.35 mol/L at ¼ L to 0.40 mol/L at ¾ L. This indicates a non-uniform distribution of reactants, with higher concentrations accumulating downstream due to limited mass transport in the upstream sections. Such a gradient suggests inefficient electrolyte delivery, leading to incomplete electrode utilization and possible local concentration polarization. The observed imbalance can cause voltage losses and contribute to premature battery degradation over repeated cycles. By contrast, the lung-shaped flow field exhibits consistently higher concentrations at each corresponding cross-section, reaching 0.413 mol/L at ¼ L, 0.448 mol/L at ½ L, and 0.472 mol/L at ¾ L. This improvement—approximately 18% higher across the board—demonstrates the superior mass transfer efficiency enabled by the lung-inspired structure. The design's branched network mimics the fractal geometry of biological systems, such as alveoli or leaf veins, effectively distributing the electrolyte throughout the porous electrode. The lung-shaped design's ability to deliver reactants uniformly results in a more homogeneous electrochemical reaction across the entire electrode surface. This not only improves energy conversion efficiency but also reduces localized wear, thereby enhancing the long-term durability and stability of the battery.

In conclusion, **Figure 8** confirms the importance of flow field architecture in determining electrolyte distribution. The biomimetic lung-shaped flow field outperforms the serpentine design by maintaining higher and more uniform V^{2+} ion concentrations at all electrode depths, making it a promising candidate for next-generation redox flow battery optimization.

Figure 9 explores the spatial distribution of V^{2+} ion concentrations across the normalized width of the porous electrode at three representative positions along its length: ¼ L, ½ L, and ¾ L, where L is the total electrode length. **Figure 9** compares this distribution for two distinct flow field configurations: the conventional serpentine flow field and the biomimetic lung-shaped flow field. In the serpentine configuration, the V^{2+} ion concentration remains relatively low and exhibits mild fluctuations across the electrode width at each section. This suggests non-uniform reactant penetration, likely due to limited flow access in certain regions. Especially near the electrode surfaces further from the flow channel, ion starvation may occur, leading to sub-optimal redox reactions and inefficient electrode usage. At ¾ L, while the concentration increases slightly, the inconsistency across the width still signals mass transport limitations, which can compromise both performance and durability. On the other hand, the lung-shaped flow field demonstrates a markedly improved and smoother concentration distribution across the same positions. Not only are the concentrations consistently higher, by approximately 18% across all cross-sections, but they also appear more evenly spread. This enhanced uniformity indicates that the lung-inspired design enables balanced flow penetration throughout the electrode width, ensuring that even the inner pores receive adequate electrolyte supply.

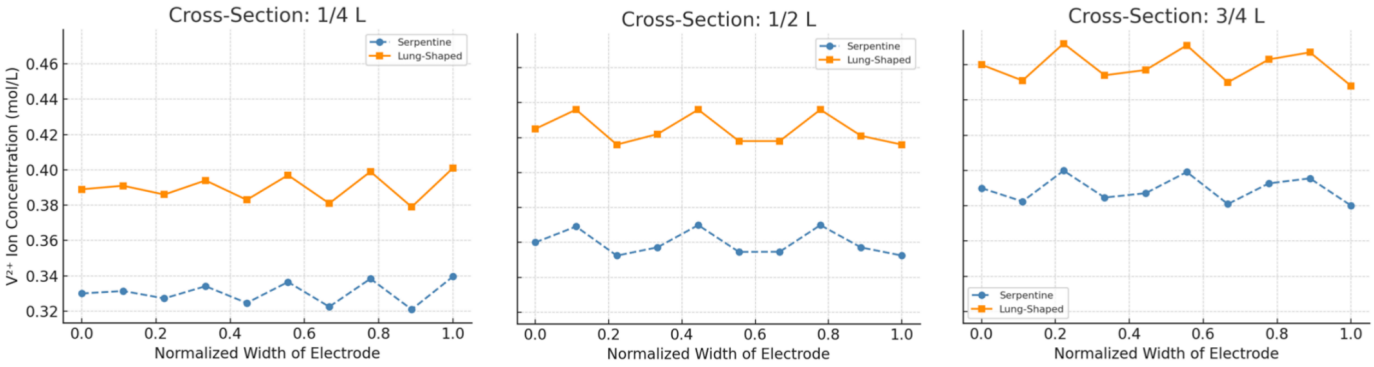

Figure 9. Crosswise V^{2+} Concentration Profiles at Three Positions Along the Porous Electrode.

The success of the lung-shaped structure lies in its biomimetic branching architecture, which resembles the vascular systems of leaves or lungs. These natural systems are optimized for distributing fluids efficiently and uniformly, a principle now applied here to improve battery performance. As a result, the lung-shaped design minimizes concentration gradients, reduces energy loss due to polarization, and allows for more complete and balanced utilization of the electrochemical surface. Overall, **Figure 9** validates that the lung-inspired flow field significantly enhances in-plane concentration uniformity within the electrode. This leads to better redox kinetics, improved energy efficiency, and increased battery lifespan. Such biomimetic engineering shows tremendous promise for revolutionizing flow battery architecture.

Figure 10 illustrates the evolution of the spatially averaged V^{2+} ion concentration within the porous electrode of a vanadium redox flow battery (VRFB) as a function of the state of charge (SOC) during discharge. It compares two distinct flow field geometries: the traditional serpentine flow field and the biomimetic lung-shaped flow field. In the case of the serpentine flow field, the average V^{2+} ion concentration shows a modest increase from 0.33 mol/L at SOC = 0.1 to 0.37 mol/L at SOC = 0.9. This gradual upward trend suggests that the system maintains a baseline level of ion availability throughout discharge. However, the relatively low concentrations and the shallow slope point to inefficient mass transport, where parts of the electrode, especially in less accessible zones, suffer from poor reactant penetration and local depletion. Such limitations can cause increased polarization, uneven current distribution, and suboptimal energy output. By contrast, the lung-shaped flow field demonstrates a consistently higher spatial average V^{2+} ion concentration across all SOC levels. Starting from approximately 0.39 mol/L at SOC = 0.1 and rising to about 0.44 mol/L at SOC = 0.9, the biomimetic design outperforms the serpentine configuration by roughly 18% at each discharge point. This considerable improvement reflects the lung-shaped design's superior capacity for uniform electrolyte distribution, ensuring that the entire electrode volume remains actively engaged in the redox process. The advantage stems from the branched, hierarchical structure of the lung-inspired channels, which mimic biological systems that efficiently distribute fluids (alveolar airways or leaf venation). These structures reduce flow resistance, eliminate dead zones, and promote equal access to reactants. As a result, the electrode's electrochemical surface is better utilized, and ion concentrations remain stable even as discharge progresses.

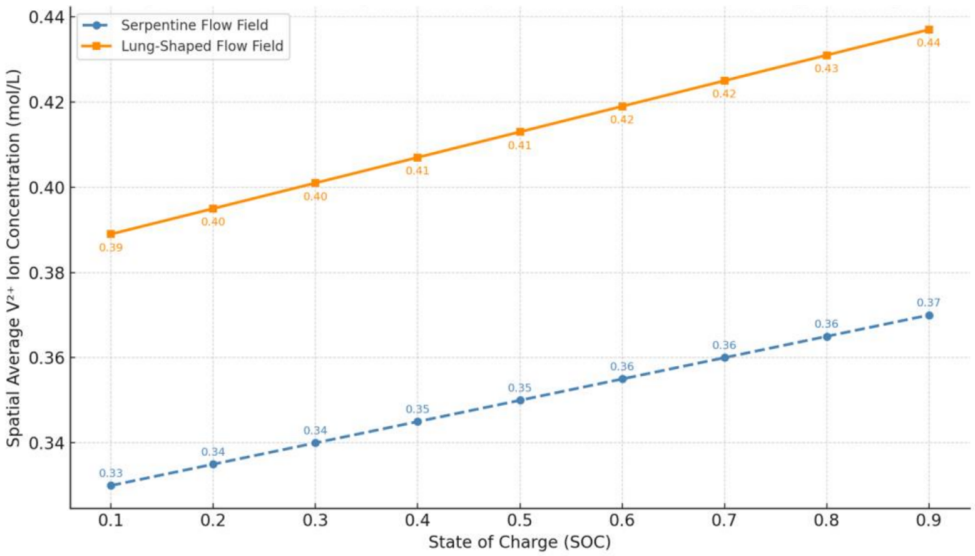

Figure 10. SOC-Dependent Behavior of Mean V^{2+} Ion Concentration in a VRFB Electrode.

In summary, **Figure 10** highlights that biomimetic flow field designs not only enhance local concentration distribution (as seen in **Figures 8** and **9**) but also maintain a higher and more stable global average concentration throughout the entire discharge cycle. This leads to greater energy efficiency, higher power density, and improved overall performance, solidifying the lung-shaped configuration as a promising advancement for the future of redox flow battery design.

Experimental results

The uniformity factor is a critical metric that quantifies how evenly the reactant ions, particularly vanadium ions, are distributed within the porous electrode. A higher value of this factor indicates better homogeneity of reactant access, which translates directly into improved electrochemical performance and reduced local overpotentials. In the traditional serpentine flow field, the uniformity factor starts at 0.45 at SOC = 0.1 and gradually increases to 0.55 at SOC = 0.9. This slow and modest improvement suggests that the serpentine geometry struggles to distribute reactants efficiently, especially at the beginning of the discharge cycle. Localized depletion of active species may occur, limiting the effectiveness of redox reactions and potentially leading to uneven current distribution and energy losses. By contrast, the lung-shaped biomimetic flow field exhibits significantly higher uniformity factors throughout the discharge process. At SOC = 0.1, the value already reaches 0.611, representing an improvement of approximately 35.6% compared to the serpentine design. As SOC increases, the lung-shaped design maintains a consistent lead, reaching 0.746 at SOC = 0.9. This consistently higher performance can be attributed to the hierarchical branching and natural gradient distribution engineered into the lung-inspired geometry, which ensures better flow dispersion and reactant accessibility across the entire electrode. This superior mass transport behavior in the lung-shaped flow field reduces concentration polarization, enhances reaction kinetics, and promotes more uniform utilization of the electrode surface. The overall result is a more efficient discharge process with reduced energy loss and improved battery performance.

In conclusion, **Table 4** highlights that biomimetic optimization of flow field

design, by mimicking natural vascular networks like those in lungs, can dramatically enhance the uniformity of species distribution. This insight has profound implications for the next generation of high-performance redox flow batteries, where maximizing electrochemical efficiency and stability is paramount.

Table 5 provides a comparative analysis of the average concentration of V^{2+} ions measured at three different cross-sectional positions ¼ L, ½ L, and ¾ L along the length of the porous electrode. This comparison is made between the conventional serpentine flow field and the biomimetic lung-shaped flow field during the discharge process of a vanadium redox flow battery (VRFB). For the serpentine flow field, the V^{2+} concentrations at the three cross-sections increase gradually from 0.35 mol/L at ¼ L to 0.40 mol/L at ¾ L. This slight upward trend indicates that ions accumulate more toward the exit of the electrode, possibly due to uneven flow distribution and limited mass transport efficiency. Such behavior often leads to under-utilization of the upstream regions of the electrode and localized ion starvation, which can compromise reaction kinetics and reduce overall battery efficiency. In contrast, the lung-shaped flow field demonstrates consistently higher concentrations at all measured cross-sections: 0.413 mol/L, 0.448 mol/L, and 0.472 mol/L respectively, representing an approximate 18% improvement over the serpentine geometry at each point. This substantial enhancement underscores the lung-shaped design's ability to deliver a more homogeneous and richer supply of active species throughout the entire electrode. The increase in concentration uniformity in the lung-inspired design can be attributed to its branching flow channels, which mimic the natural efficiency of biological systems such as respiratory and vascular networks. These channels facilitate a more even and directed flow of electrolyte, improving ion accessibility and reducing the formation of stagnant zones. As a result, the electrode surface is utilized more evenly, and the redox reactions proceed more efficiently across all regions.

Table 5. Average Vanadium Ion (V^{2+}) Concentration at Selected Electrode Cross-Sections.

Cross-section	Serpentine flow field uniformity factor	Lung-shaped flow field uniformity factor
1/4 L	0.35	0.413
1/2 L	0.38	0.448
3/4 L	0.4	0.472

This table therefore demonstrates that the lung-shaped flow field achieves not only higher average concentrations of V^{2+} ions but also a more balanced spatial distribution. This directly contributes to better discharge performance, reduced polarization losses, and longer system durability. The findings emphasize the critical role of geometrical design in optimizing mass transfer, and they support the integration of biomimetic principles into the engineering of next-generation energy storage devices.

Table 6 details the distribution of vanadium ion (V^{2+}) concentrations across the normalized width of the porous electrode at three longitudinal position, ¼ L, ½ L, and ¾ L, comparing the performance of the serpentine and lung-shaped flow fields. This information is crucial for understanding how effectively the electrolyte penetrates the porous matrix and delivers reactants to the active sites throughout the electrode depth. At all three cross-sectional positions, the serpentine flow field exhibits a

slightly fluctuating and generally lower concentration profile. For example, at ¼ L, V^{2+} concentrations range narrowly around 0.33–0.35 mol/L, with mild oscillations due to uneven flow dynamics and possible stagnation zones. This suggests that the serpentine channels struggle to maintain uniform reactant penetration through the electrode thickness, which can lead to under-utilization of the inner pore structure and loss in electrochemical efficiency. In contrast, the lung-shaped flow consistently delivers higher and more uniform concentration values across the same spatial domain. The lung-mimicking structure ensures smoother electrolyte dispersion, resulting in V^{2+} concentration levels that are roughly 18% higher at every corresponding location. At ½ L, for instance, the lung-inspired design maintains concentrations between 0.43 and 0.46 mol/L, highlighting its superior ability to feed ions evenly from the flow channels into the entire electrode volume. This clear improvement in spatial homogeneity is attributed to the biomimetic architecture of the lung-shaped design, which mimics the fractally branching networks seen in natural systems such as bronchi or leaf veins. These structures are evolutionarily optimized to distribute fluids efficiently and uniformly, and when applied to redox flow batteries, they dramatically enhance mass transport characteristics. The reduced concentration gradients lead to lower polarization, better electrode utilization, and improved current distribution. Thus, **Table 6** reinforces that geometry-driven flow optimization can play a transformative role in advancing energy storage systems. The lung-shaped design not only raises the absolute values of ion concentration within the electrode, but also minimizes variation across its depth offering a more stable and efficient platform for redox reactions.

Table 6. Transversal Distribution of V^{2+} Ions at Multiple Locations Along the Electrode Length.

Electrode width	1/4 L-serpentine (mol/L)	1/4 L-lung-shaped (mol/L)	1/2 L–serpentine (mol/L)	1/2 L-lung-shaped (mol/L)	3/4 L–serpentine (mol/L)	3/4 L-lung-shaped (mol/L)
0.0	0.33	0.389	0.36	0.425	0.39	0.46
0.1	0.331	0.391	0.369	0.436	0.382	0.451
0.2	0.327	0.386	0.352	0.416	0.4	0.472
0.3	0.334	0.394	0.357	0.422	0.385	0.454
0.4	0.325	0.383	0.37	0.436	0.387	0.457
0.6	0.337	0.397	0.355	0.418	0.399	0.471
0.7	0.322	0.381	0.355	0.418	0.381	0.45
0.8	0.338	0.399	0.37	0.436	0.393	0.463
0.9	0.321	0.379	0.357	0.421	0.396	0.467
1.0	0.34	0.401	0.352	0.416	0.38	0.448

Table 7 showcases the evolution of the spatial average concentration of V^{2+} ions within the porous electrode as a function of the state of charge (SOC) during the discharge cycle of a vanadium redox flow battery (VRFB). This metric offers a global perspective on how efficiently active species are transported and maintained across the electrode structure over the course of battery operation. For the serpentine flow field, the spatial average concentration of V^{2+} ions gradually increase from 0.33 mol/L at SOC = 0.1 to 0.37 mol/L at SOC = 0.9. While this upward trend reflects some level of reactant retention as the battery discharges, the overall growth is modest. The serpentine geometry, with its linear and constrained channel design, limits the uniform delivery of electrolyte and can create concentration gradients and localized

depletion, especially in deeper or peripheral electrode regions. This ultimately hinders the effective utilization of the electrode's reactive surface area. In contrast, the lung-shaped flow field demonstrates consistently higher spatial average concentrations at each stage of the discharge process. Starting at ~0.39 mol/L for SOC = 0.1 and reaching ~0.44 mol/L at SOC = 0.9, the lung-inspired geometry outperforms its conventional counterpart by approximately 18% across all SOC levels. This enhanced performance reflects the superior electrolyte management enabled by the lung-shaped design, which emulates natural branching networks such as the pulmonary system or leaf venation. By promoting even distribution and continuous access of active species throughout the electrode volume, the lung-shaped configuration reduces local depletion zones, minimizes concentration polarization, and sustains redox activity more uniformly. This results in better electrochemical kinetics, higher power output, and more stable operational characteristics throughout the battery's discharge phase. The implications of this comparison are significant. The table reveals that flow field architecture plays a critical role not only in spatial distribution but also in maintaining overall system health and efficiency. The biomimetic lung-shaped flow field stands out as a high-potential design for future VRFBs, capable of supporting higher ion utilization and more effective energy delivery.

Table 7. Discharge-Driven Trends in Averaged V^{2+} Ion Concentration vs. Charge State.

Ref.	State of charge (SOC)	Serpentine flow field avg. V^{2+} Conc. (mol/L)	Lung-shaped flow field avg. V^{2+} Conc. (mol/L)
1	0.3	0.330	0.389
2	0.4	0.335	0.395
3	0.3	0.340	0.401
4	0.4	0.345	0.407
5	0.5	0.350	0.413
6	0.6	0.355	0.419
7	0.7	0.360	0.425
8	0.8	0.365	0.431
9	0.5	0.370	0.437
10	0.1	0.330	0.389

4.3. Output characteristic

In this subsection, the output characteristics of the vanadium redox flow battery (VRFB) are assessed under two different flow field geometries: the conventional serpentine channel and the biomimetic lung-shaped design. The main metric of comparison is the polarization curve, which reflects the relationship between current density and output voltage during the discharge process a fundamental indicator of the battery's electrochemical performance. The serpentine flow field, although widely used in conventional designs, exhibits notable limitations. As the current density increases, the output voltage declines sharply due to a combination of ohmic resistance, activation losses, and more prominently, concentration polarization. This steep voltage drop suggests that the serpentine structure fails to supply adequate electrolyte uniformly throughout the electrode at higher operational rates. As a result, localized ion depletion and incomplete electrode utilization reduce the energy output, particularly under high load conditions. In contrast, the lung-shaped flow field demonstrates a significantly

more favorable output profile. The polarization curve corresponding to this design shows a slower and more gradual voltage decay with increasing current density. This indicates that the system maintains better access to active species across the electrode surface, ensuring more uniform redox activity and reduced performance degradation even at elevated operating rates. The key factor behind this improved behavior lies in the efficient and hierarchical branching geometry of the lung-inspired flow field. By mimicking biological fluid distribution networks, such as pulmonary airways or leaf venation, the design promotes even electrolyte distribution, minimizes dead zones, and shortens diffusion paths within the porous electrode. This results in lower internal resistance and a more balanced reaction environment, thereby enhancing both energy efficiency and power density. Furthermore, the lung-shaped configuration supports enhanced species utilization, as confirmed in earlier subsections by its superior ion concentration profiles and uniformity factor. These improvements collectively translate into higher discharge voltages, better stability, and a longer operational range—all critical metrics for real-world energy storage systems.

In summary, the output characteristic analysis confirms that the lung-shaped flow field outperforms the serpentine design not only at the microstructural (mass transfer) level but also in terms of overall battery functionality. This makes it a promising candidate for scalable, high-efficiency redox flow battery systems, especially under demanding energy and power conditions.

Figure 11 illustrates the polarization curves of the VRFB under two different flow field geometries: the traditional serpentine and the biomimetic lung-shaped flow field. A polarization curve is a fundamental diagnostic tool that plots cell voltage versus current density, revealing how different loss mechanisms ohmic, activation, and concentration affect the battery's output performance as the current demand increases. In the serpentine flow field, the curve exhibits a steeper decline in voltage as current density rises. At low current densities, the voltage remains relatively high, dominated by activation polarization associated with the initiation of electrochemical reactions. However, as the current density increases, ohmic resistance and concentration polarization become more prominent. The limited mass transport in the serpentine channels leads to non-uniform reactant distribution, causing local depletion zones that accelerate voltage losses. This steep voltage drop signifies reduced operational stability and efficiency at high discharge rates. In contrast, the lung-shaped flow field produces a more favorable polarization profile, with higher voltages sustained across the entire current density range. The voltage decay is more gradual, indicating lower ohmic and concentration losses. This performance improvement arises from the hierarchical branching architecture of the lung-inspired channels, which ensures even electrolyte distribution throughout the electrode. By eliminating stagnation zones and enhancing mass transfer, the lung-shaped design allows the redox reactions to proceed more uniformly, which directly translates to higher energy conversion efficiency and greater power density. The gap between the two curves widens with increasing current density, emphasizing that the lung-shaped flow field offers significant advantages under high-load conditions. This characteristic is crucial for practical VRFB applications, where batteries are expected to sustain stable

operation and high output without excessive voltage losses.

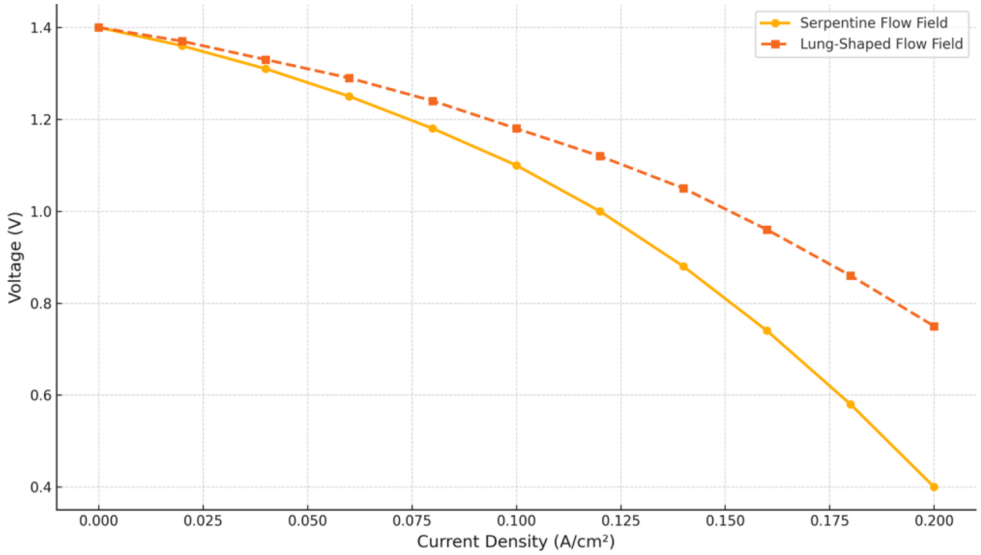

Figure 11. Comparison of Polarization Curves for Two Distinct Flow Field Geometries in VRFB.

In summary, **Figure 11** clearly demonstrates that the biomimetic lung-shaped flow field significantly enhances the polarization behavior of VRFBs, reducing energy losses, improving high-current performance, and maximizing electrode utilization. This confirms that biomimetic flow field optimization is a powerful strategy for advancing next-generation, high-efficiency redox flow batteries.

Figure 12 displays the power density curves corresponding to two flow field architectures: the conventional serpentine flow field and the biomimetic lung-shaped flow field. The graph shows how the output power density (W/cm²) evolves with increasing current density (A/cm²), a critical indicator of the battery's ability to deliver high power efficiently under varying load conditions. In the case of the serpentine flow field, the power density increases initially as the current density rises, reaching a peak before gradually declining. The maximum power density is relatively low, and the curve shows a narrow plateau. This behavior reflects the typical performance limitation of the serpentine design, where reactant delivery becomes insufficient at higher current loads due to uneven electrolyte distribution and mass transport constraints. As current continues to rise, the voltage drop becomes more pronounced (as seen in the polarization curve), leading to a sharp decline in power output beyond the optimal operating point. Conversely, the lung-shaped flow field achieves a higher maximum power density, and the curve features a broader and flatter peak. This improvement highlights the lung-inspired design's ability to sustain high performance over a wider range of current densities. The branching channel network, inspired by biological systems such as the human respiratory system, provides more uniform access to the active sites across the porous electrode. This leads to enhanced electrolyte utilization, minimized local depletion, and reduced internal resistance—all of which contribute to smoother and more efficient power output. Importantly, the lung-shaped design not only raises the peak power density but also shifts the optimal current density window, allowing the battery to operate efficiently at higher loads. This makes it more suitable

for applications demanding dynamic performance or high-power pulses, such as grid balancing or fast charging systems.

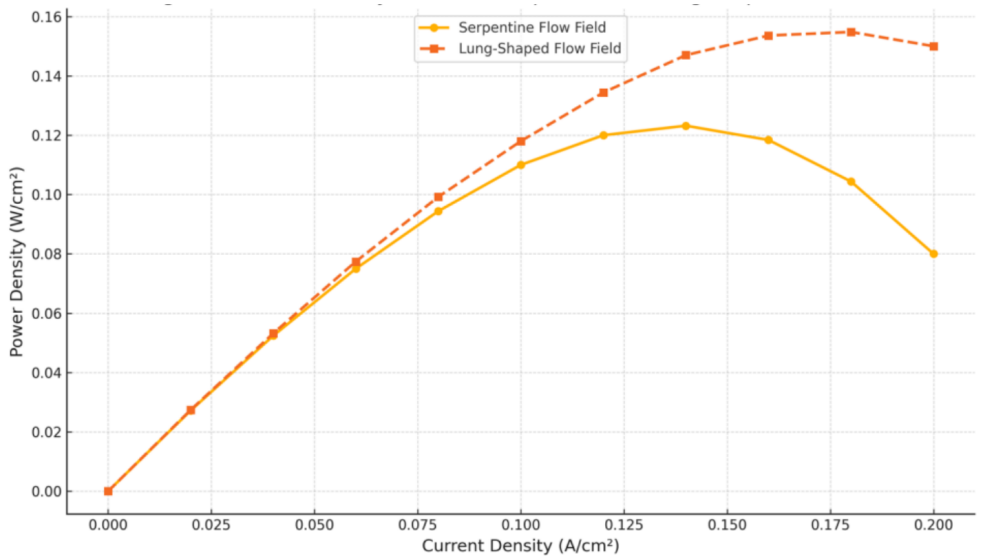

Figure 12. Effect of Flow Field Geometry on Power Density in Vanadium Redox Flow Battery.

In conclusion, **Figure 12** clearly demonstrates the lung-shaped flow field's superior ability to enhance power output in redox flow batteries. By ensuring efficient mass transport and improving current distribution, it supports higher, more stable power delivery, establishing it as a highly promising geometry for high-performance, scalable energy storage systems. The superior performance of the lung-shaped flow field underscores a critical advancement over prior biomimetic approaches. While previous branching designs improved hydraulic distribution, our lung-inspired architecture specifically targets the core mass transport limitation in VRFBs: volumetric reactant delivery. The fractal, volume-filling nature of the lung pattern, as opposed to the more 2D nature of leaf venation, is the key differentiator. This is quantitatively evidenced by the 18% higher average V^{2+} concentration at the ¾ L cross-section and the 35.6% improvement in flow uniformity. These metrics confirm that our design successfully facilitates deeper electrolyte penetration and more uniform active species distribution across the electrode depth, directly addressing the research gap of electrode under-utilization and localized depletion that persists in even advanced conventional and biomimetic flow fields. The performance superiority of the lung-shaped flow field can be attributed to its specific architectural advantages over other biomimetic designs. While leaf-inspired and other branching patterns improve upon conventional layouts, they are often optimized for 2D surface coverage. In contrast, the 3D hierarchical, volume-filling nature of the lung-inspired pattern, mimicking the pulmonary acinus, is fundamentally tailored to facilitate efficient mass transport through the depth of the porous electrode. This results in a more uniform active species distribution and a significant reduction in concentration polarization, as evidenced by the 35.6% higher uniformity factor and 18% greater ion concentration reported herein. This highlights that the choice of biological analog and its adaptation for the specific physics of the VRFB electrode are critical for maximizing performance gains.

5. Conclusions

This study introduced a novel biomimetic lung-inspired flow field design for all-vanadium redox flow batteries (VRFBs), evaluated through a detailed three-dimensional numerical simulation in comparison to the conventional serpentine flow field. The findings highlight the superior electrochemical and hydrodynamic performance of the proposed structure. Specifically, the lung-shaped flow field achieved a 9.77% increase in discharge voltage at SOC = 0.1 and required 5.34% less charging voltage at SOC = 0.9, indicating reduced energy losses and enhanced round-trip efficiency. Furthermore, the electrolyte concentration uniformity, characterized by the uniformity factor, improved by 35.6%, demonstrating a more homogenous ion distribution that minimizes concentration polarization. A significant improvement in mass transport behavior was also observed: the average V^{2+} ion concentration at the ¾-length cross-section increased by 18% compared to the serpentine counterpart. This enhancement reflects the flow field's capacity to facilitate efficient ionic diffusion and reaction kinetics across the porous electrode. Additionally, the reduction in pressure drop directly contributed to higher net discharge power and improved power-based efficiency, reinforcing the flow field's potential for energy-saving operation. In summary, the biomimetic lung-shaped flow field significantly enhances VRFB performance by optimizing ionic distribution, minimizing energy losses, and improving overall electrochemical efficiency. This advancement offers a promising design strategy for the next generation of high-efficiency flow battery systems tailored for large-scale energy storage applications.

Author contributions: The author confirm contribution to the paper as follows: Conceptualization, JH and LA; validation, JH, LA and CH; formal analysis, JH and CH; investigation, JH, LA and CH; resources, JH and LA; data curation, CH and AK; writing—original draft preparation, JH, LA and MB; writing—review and editing, JH, AK and MB; visualization, JH and MB.; supervision, JH, AK and MB; project administration, AK and MB; funding acquisition, LA. All authors have read and agreed to the published version of the manuscript.

Funding: This research was funded by the Deanship of Scientific Research of Taif University, grant number 83/ Deanship-of-Scientific-Research, and the APC was funded by the Deanship of Scientific Research of Taif University (DSRTU).

Institutional review board statement: Not applicable.

Informed consent statement: Not applicable.

Data availability statement: Not applicable.

Acknowledgment: The author would like to acknowledge the Taif University Department of Scientific Research in the Kingdom of Saudi Arabia for assistance and motivation to accomplish the research work.

Conflict of interest: The authors declare no conflicts of interest to report regarding the present study.

References

1. Xu Q, Zhao TS, Leung PK. Numerical investigations of flow field designs for vanadium redox flow batteries. Applied Energy. 2013; 105: 47–56. doi: 10.1016/j.apenergy.2012.12.041
2. Wang Q, Qu ZG, Jiang ZY, et al. Numerical study on vanadium redox flow battery performance with non-uniformly compressed electrode and serpentine flow field. Applied Energy. 2018; 220: 106–116. doi: 10.1016/j.apenergy.2018.03.058
3. Ha J, Kim S, Kim Y, et al. Capacity fade-aware parameter identification of zero-dimensional model for vanadium redox flow batteries. Applied Energy. 2025; 380: 124989. doi: 10.1016/j.apenergy.2024.124989
4. Lu M-Y, Yang W-W, Bai X-S, et al. Performance improvement of a vanadium redox flow battery with asymmetric electrode designs. Electrochimica Acta. 2019; 319: 210–226. doi: 10.1016/j.electacta.2019.06.158
5. Yang WW, Bai XS, Zhang WY, et al. Numerical examination of the performance of a vanadium redox flow battery under variable operating strategies. Journal of Power Sources. 2020; 457: 228002. doi: 10.1016/j.jpowsour.2020.228002
6. Wang J, Chen J, Zhou G, et al. Experimental study on vanadium redox flow battery performance under asymmetric electrolyte flow configuration. Journal of Energy Storage. 2025; 145: 119862. doi: 10.1016/j.est.2025.119862
7. Yue M, Zheng Q, Xing F, et al. Flow field design and optimization of high power density vanadium flow batteries: A novel trapezoid flow battery. AIChE Journal. 2018; 64(2): 782–795. doi: 10.1002/aic.15959
8. Chu F, Xiao G, Xia L, et al. Analysis of battery performance and mass transfer behavior for organic redox flow battery with different flow fields. Journal of The Electrochemical Society. 2022; 169(7): 070529. doi: 10.1149/1945-7111/ac81f4
9. Skyllas-Kazacos M, Goh L. Modeling of vanadium ion diffusion across the ion exchange membrane in the vanadium redox battery. Journal of Membrane Science. 2012; 399–400: 43–48. doi: 10.1016/j.memsci.2012.01.024
10. Bogdanov S, Ibanez FM, Sun C, et al. Non-isothermal modeling of vanadium redox flow battery for low-temperature conditions. Journal of Power Sources. 2025; 653: 237721. doi: 10.1016/j.jpowsour.2025.237721
11. Knehr KW, Agar E, Dennison CR, et al. A transient vanadium flow battery model incorporating vanadium crossover and water transport through the membrane. Journal of The Electrochemical Society. 2012; 159(9): A1446–A1459. doi: 10.1149/2.017209jes
12. Fu S, Liu R, Guan C, et al. Enhancing TiO^{2+}/Ti^{3+} redox kinetics by nitrogen-doped carbon nanofiber composite electrodes for titanium-cerium flow batteries. Electrochimica Acta. 2025; 542: 147421. doi: 10.1016/j.electacta.2025.147421
13. Oh K, Yoo H, Ko J, et al. Three-dimensional, transient, nonisothermal model of all-vanadium redox flow batteries. Energy. 2015; 81: 3–14. doi: 10.1016/j.energy.2014.05.020
14. Lin C, Gao Y, Li N, et al. Quaternized Tröger's base polymer with crown ether unit for alkaline stable anion exchange membranes. Electrochimica Acta. 2020; 354: 136693. doi: 10.1016/j.electacta.2020.136693
15. Fan L, Zhu B, Chen M, et al. High performance transition metal oxide composite cathode for low temperature solid oxide fuel cells. Journal of Power Sources. 2012; 203: 65–71. doi: 10.1016/j.jpowsour.2011.12.017
16. Wang Q, Shan X, Liu H, et al. Mass transfer in micro-nano porous electrodes: A crucial role in optimizing vanadium redox flow battery performance. Journal of Colloid and Interface Science. 2025; 705: 139465. doi: 10.1016/j.jcis.2025.139465
17. Kumar S, Jayanti S. Effect of flow field on the performance of an all-vanadium redox flow battery. Journal of Power Sources. 2016; 307: 782–787. doi: 10.1016/j.jpowsour.2016.01.048
18. Gundlapalli R, Jaiswal G. Adapting serpentine flow fields for application in large-scale vanadium redox flow battery cells through marginal design modifications. Journal of Power Sources. 2025; 657: 238231. doi: 10.1016/j.jpowsour.2025.238231
19. Zhou Z, Ren Y, Yu F, et al. Monolithic low-tortuous copper(I) phosphide nanorod arrays for exceptional areal performance in electrochemical chloride ion removal. Nano Energy. 2025; 137: 110792. doi: 10.1016/j.nanoen.2025.110792
20. Kumar S, Jayanti S. Effect of electrode intrusion on pressure drop and electrochemical performance of an all-vanadium redox flow battery. Journal of Power Sources. 2017; 360: 548–558. doi: 10.1016/j.jpowsour.2017.06.045
21. Jyothi N, Prabu S, Joo SW, et al. Synergistic integration of Co9S8 and WO3 nanotube clusters via rational

hydrothermal engineering for enhanced supercapacitor performance. Journal of Alloys and Compounds. 2025; 1048: 185362. doi: 10.1016/j.jallcom.2025.185362

22. Bhosale NY, Mali SS, Hong CK, et al. Hydrothermal synthesis of WO_3 nanoflowers on etched ITO and their electrochromic properties. Electrochimica Acta. 2017; 246: 1112–1120. doi: 10.1016/j.electacta.2017.06.142
23. Yu Y, Hu G, Liu C, et al. Prediction of solar irradiance one hour ahead based on quantum long short-term memory network. IEEE Transactions on Quantum Engineering. 2023; 4: 1–15. doi: 10.1109/TQE.2023.3271362
24. Ensafi AA, Abarghoui MM, Rezaei B. Facile synthesis of Pt-Cu@silicon nanostructure as a new electrocatalyst supported matrix, electrochemical detection of hydrazine and hydrogen peroxide. Electrochimica Acta. 2016; 190: 199–207. doi: 10.1016/j.electacta.2015.12.180
25. Athanasiou M, Niakolas DK, Bebelis S, et al. Steam effect on Gerischer impedance response of a Ni/GDC|YSZ|LSM fuel cell /anode. Journal of Power Sources. 2020; 448: 227404. doi: 10.1016/j.jpowsour.2019.227404